ELASTIC PULSED WAVE PROPAGATION IN MEDIA WITH SECOND OR HIGHER ORDER NONLINEARITY.

PART II: SIMULATION OF EXPERIMENTAL MEASUREMENTS ON BEREA SANDSTONE.

Koen E-A Van Den Abeele

Post-Doctoral Research Fellow, EES-4, MS D443, Los Alamos National Laboratory, Los Alamos, NM 87545, USA.

also Post-Doctoral Fellow of the Belgian Foundation for Scientific Research, K.U.Leuven Campus Kortrijk, Interdisciplinary Research Center, E. Sabbelaan 53, B-8500 Kortrijk, Belgium.

ABSTRACT

We apply the theoretical 1D wave propagation model described in Part I to laboratory data from dynamic propagating wave experiments on a 2 meter long cylindrical rod of Berea sandstone as previously reported by Meegan et al.[1] Using the iterative procedure, good agreement is obtained limiting model parameters up to cubic anharmonicity (i.e. 2 nonlinear terms proportional to β and δ in the stress-strain polynomial expansion). Both the data and simulations illustrate that nonlinear response is likely to occur even at extremely small strains (order 10^{-7}). As generally expected for disordered materials, the resulting values for the nonlinear parameters are several orders of magnitude larger than those for intact (uncracked, non-compliant) materials. We discuss the values obtained for the dynamic nonlinearity parameters in relation to commonly obtained static and resonance results which suggest the need to include more complicated phenomena such as hysteresis in the theory.

INTRODUCTION

Elastic nonlinear behavior in rocks may manifest itself in a variety of manners (nonlinear stress-strain equation with or without hysteresis, nonlinear attenuation, harmonic generation, resonant peak shift) and can be observed in several different ways (static and quasi-static tests, torsional oscillator experiments, Young's mode resonance experiments, dynamic pulse mode experiments). (See the review by Johnson and Rasolofosaon[2] for references to each individual technique). The mechanism responsible for this nonlinear behavior is believed to be due to the presence of compliant features and the influence of fluid[3].

In this paper we focus on dynamic pulse wave propagation and apply the theoretical model described in Part I to simulate previously reported experiments conducted by Meegan et al.[1] (MJGM in remainder of text) on Berea Sandstone. In the first section we briefly review the experimental setup used in the nonlinear measurements as applied by MJGM. We then discuss the experimental data and simulations using the 1D model described in Part I. Different attenuation models are contrasted and compared in the calculations. We also show typical signal distortion based on the parameters resulting from the simulation. The dynamic values for the nonlinearity coefficients differ to some extent from the ones obtained in static stress-strain measurements and resonance experiments. We comment on this difference in the final section, and suggest alternative theories which might account for this difference.

EXPERIMENTAL SETUP

The experiment is described in detail by Meegan et al.[1] A 2 m long, 6 cm diameter, cylindrical sample of Berea sandstone was used in the experiment (see Figure 1). Source frequencies of 8 to 24 kHz were used, and detectors (pinducers) were embedded in the rod at pre-determined intervals. The source displacement was measured by use of an optical probe.

DATA AND SIMULATION

MJGM Results.

At ambient conditions, time-of-flight measurements yield a linear sound speed in the Berea Sandstone bar of about 2600 m/s, and, in the absence of the receiving pinducers, a value of about 60 for Q_L was reported. One experimental observation originally shown by MJGM providing evidence for the nonlinear response of the rock is shown in Figure 2. In Figure 2a the spectral composition of the displacement of the source transducer (measured by the displacement probe) while being driven at 13.75 kHz is illustrated. The five different curves correspond to five amplitudes of the source transducer varying over a factor of approximately 50. Note that, as the amplitude at the fundamental (drive) frequency was increased, the amplitude at frequencies other than the drive frequency remained very low (the 2ω harmonic (where ω is angular frequency) is down by approximately two orders of magnitude from the fundamental and no higher harmonics are observed). As reproduced in Figure 2b, MJGM illustrated the spectral composition for the five drive amplitudes after the signal had propagated 58 cm (about three wavelengths of the fundamental) from the source transducer. Comparison of parts (a) and (b) of Figure 2 reveals the presence of rich harmonic content at 58 cm that does not exist at the source.

In their paper, MJGM approximately verified the three fundamental relations predicted by the 1-D perturbation theory derived by McCall.[4] These include: the displacement amplitude of the second harmonic (A_2) grows linearly with propagation distance (using spectral ratios); A_2 shows a quadratic dependence on the fundamental source amplitude; and A_2 grows with a quadratic dependence on source frequency ω ($=2\pi f$).

The iterative theoretical model described in Part I is a more powerful approach than the basic perturbation results used by MJGM. This is because, 1) the method can account for the entire frequency spectrum (i.e. harmonics higher than 2ω and 3ω); 2) use of numerous iterations leads to more accurate results and functional dependencies (i.e., energy is approximately conserved); and 3), attenuation effects can be considered.

Application of the new Theoretical Approach.

We tested the new model in a reduced form limiting ourselves to the weighting interaction functions W_1 and W_2 in the generalized solution of the nonlinear equation (i.e. second order approximation $u = u_0 + u_1 + u_2$). Given the drive frequency (f=13.75 kHz), the total travel distance (L=58 cm) and a measured value for the linear speed (c_o=2600 m/s), we performed simulations of the 1-D wave propagation in β-δ parameter space. In a first attempt we used an estimation for the linear attenuation relation in a sandstone bar with Q_L=60, corresponding to the medium constant for the sandstone bar in ambient conditions and in the absence of the receiving pinducers. We reproduced the MJGM observed spectra at the various source amplitudes to very good agreement using the following values: β'=-250 and δ'=-3.2·10^8 or equivalently β=-500 and δ=-9.6·10^8 (the primes indicate MJGM and McCall[4] notation; the unprimed values are the classical nonlinear acoustics values).

The comparison between the theoretical predictions and the experimental data are shown in Figure 3. Each of the drive levels corresponding to those shown in Figure 2 are shown by a

separate spectral plot. The simulation was performed using 20 iterations, equivalent to 20 distance steps of 2.9 cm. Except for the input intensity, all model parameters (input frequency, sound velocity, attenuation, distance and both nonlinear coefficients) are kept constant in the simulations. The amplitudes and frequencies of the simulations are indicated by the vertical arrows in the figures. The amplitudes of the harmonics show good agreement with the experimental data for all levels of source intensity. On the other hand, the predicted amplitude of the fundamental component at 58 cm is always higher than the measured value. This implies that attenuation must be much larger than expected, especially considering the fact that the source intensity taken as input in the program is moderately lower than the actual data from the fiber optic probe.

A qualitative explanation for the excess attenuation has been suggested in the appendix of MJMG relating the apparently lower Q to the presence of a periodic sequence of scatterers (the eleven receivers were imbedded in the rock at intervals of 5 cm). A simple scattering model applied by MJGM illustrated that the rock with intrinsic Q_L of about 50 can be altered to an apparent Q_L of about 10 due to wave scattering. This appears to be a direct result of imbedding of the pinducers in the sample. We therefore performed the simulation again in the case of Q_L=10. The result, shown in the same manner as for the previous figure, is shown in Figure 4 using 200 iterations. The input intensity in all cases identically equals the level recorded by the optical probe at the source. We found it necessary to allow the values for β and δ to float within predetermined bounds during the simulation in order to identically match the observations. The coefficients seem to be systematically growing as a function of input level. We will return to this later. Compared to the results for Q_L=60, we note far better agreement with the measurements, especially for the fundamental component. Imbedding the pinducers indeed has had significant consequences on the dissipative nature of the medium.

To illustrate one strength of the iteration technique, we show in Figure 5 simulation results at the highest input amplitude using a single iteration, i.e. direct calculation over a single step (one iteration) of 58 cm. The identical nonlinearity parameters were used as those in the highest drive level in Figure 4 (top right, Figure 4). In the case of a single iteration, only three spectral components can be modeled as opposed to the entire spectrum. Additionally, the spectral intensity of each component is much too high since attenuation effects enter the model significantly only after a few iterations.

Even in the presence of numerous iterations, the model predicts incorrect results when only one nonlinear parameter is used. To illustrate this, Figure 6 shows the results for first order approximation by limiting calculations to $u = u_0 + u_1$, which is equivalent to considering only the influence of β. Comparison to the top right plot in Figure 4 clearly emphasizes the importance of the higher order δ-term in the observations.

Using complex representations for each frequency component, the full spectrum (amplitude and phase) and consequently the corresponding waveform can be obtained at any position from the source. Calculated waveforms at 58 cm, corresponding to the spectra shown in Figure 4, are plotted in Figure 7 for displacement and acceleration. Depending on the type of experiment, either displacement or acceleration is measured by our group. Each of the five drive levels are shown.

The distortion in the acceleration is more obvious since each spectral component is multiplied by ω^2 compared to the corresponding frequency displacement component. Although time series of waveforms for the data discussed here are not at our disposal, work by our group indicates that these waveforms exhibit the typical signal distortion response observed in our ongoing pulse investigations and nonlinear resonance experiments (e.g., Ten Cate et al.[5]; Johnson et al.[6]).

DISCUSSION

The values obtained for the first and second nonlinearity parameters β and δ are several order of magnitude larger than those found in uncracked materials, which range typically between 3 and 15 for β and with the magnitude of δ in general of the order β^2 [i.e. $\delta/\beta^2 = 1$] (e.g., Johnson and Rasolofosaon[7]). The simulation for the data discussed in this paper yield a ratio of δ to β^2 between 1600 and 6800. This relationship illustrates that rock and other compliant materials are particularly nonlinear and care must be taken when modeling the nonlinear response of these materials.

It is noteworthy that odd harmonics dominate the even harmonics in this example, and this has also been noted in resonant bar experiments (e.g., Johnson et al.[6]). Figure 4 already illustrated that the δ-term contributes as an indispensable correction to the nonlinear state relation. Recently, Na and Breazeale reported similar abnormally high third harmonics in PZT ceramics.[8-9] This feature has been related to the non-negligible influence of the fourth order elastic constants as well. Calculations by Van Den Abeele and Breazeale[9] yield ratios of δ to β^2 for various PZT-samples ranging from 127 to 15500.

Classical Theory and Hysteresis

The values of β and δ obtained from the theoretical simulation for the MJGM experiment are in disagreement with static stress-strain (and also with resonance results, e.g. Johnson et al.[6]) The first nonlinearity parameter β is roughly the same order of magnitude as that predicted by static measurements, but δ is at least 2 orders of magnitude higher than our measurements of static modulus-strain data (e.g., Guyer et al.[10]). This is a classical result for rock.

The recently developed model of Guyer et al.[10] and McCall and Guyer[11], which includes hysteresis and discrete memory in stress-strain space, predicts considerably lower values for δ in similar materials than does the theory presented here. Static measurements indicate that the nonlinear parameters increase significantly for small stress deviations compared with large static stress deviations. This observation has been reported by several authors.[10-13] Typical stress-strain behavior for large (static) and small (dynamic) excursions are visualized in Figure 8. Irrespective of the bi-functional behavior of the curves, we note that the mean hysteresis loop is steeper in the case of the small pressure deviation than in the static experiment. This is an indication of higher values for the nonlinearity parameters at smaller pressure excursions. Therefore, a distinction between dynamic and static nonlinearity parameters appears appropriate and justifies the anomaly between our model prediction and the static measurement results to a certain extent.

Are elastic pulse-mode waves hysteretic as well?

The fact that the simulation for Q_L =10 (Figure 4) yields values for both nonlinearity parameters that grow systematically with the source amplitude may be a manifestation of hysteretic behavior. The question remains as to whether the exceptional nonlinearity in earth materials as obtained from dynamic experiments is ascribed to the presence of extreme fourth (and maybe higher) order nonlinear medium constants, to hysteresis, or to a combination of both. This investigation, both theoretically and experimentally, is continuing.

CONCLUSION

The 1-D nonlinear propagation model, assuming a third order polynomial expansion of the stress-strain relation, is capable of reproducing observed experimental data for a rock (Berea sandstone) and of inferring dynamic values for the characterization of material nonlinearity. The simulation of the complete frequency spectrum is possible using an iterative procedure including attenuation and at least two nonlinearity parameters. The nonlinear parameters for Berea sandstone derived by the model are several orders of magnitude higher than found in non-compliant materials indicating that this material (and more generally all (?) rocks) exhibit highly nonlinear behavior. The modeling requires inclusion of a very large value for the second order nonlinearity parameter δ. The relation for these values to other (static) estimations is still a topic of discussion and suggest consideration of other nonlinear material behavior such as hysteresis.

Because the effects certainly are significant in rocks, accurate measurement of nonlinear contributions along the propagation path due to non-negligible higher order elastic constants or hysteresis effects may ultimately be used as a sensitive measure of consolidation and saturation in earth materials as well as symptoms of fatigue or damage.

ACKNOWLEDGMENTS

The author is indebted to P.A. Johnson for constructive review of the manuscript. The author also thanks K.R. McCall, R.A. Guyer, J.A. Ten Cate, T.J. Shankland and A. Kadish for helpful discussions and valuable comments. This research is supported by the Office of Basic Energy Science, Engineering and Geoscience under contract W7405-ENG-36 with Los Alamos National Laboratory.

REFERENCES

[1] G.D. Meegan, P.A. Johnson, R.A. Guyer and K.R. McCall, "Observations of nonlinear elastic wave behavior in sandstone", J. Acoust. Soc. Am. **94** (6), 3387-3391, Dec. 1993.

[2] P.A. Johnson and P. Rasolofosoan, "Manifestation of Nonlinear Elasticity in Rock: Convincing Evidence over Large Frequency and Strain Intervals from Laboratory Studies", Nonlinear Geophysics, 1995 (*in review*).

[3] G.A. Gist, "Fluid Effects on Velocity and Attenuation in Sandstone", J. Acoust. Soc. Am. **96** (2), 1158-1173, 1994.

[4] K.R. McCall, "Theoretical study of nonlinear elastic wave propagation", J. Geoph. Res. **99** (B2), 2591-2600, Feb. 10, 1994.

[5] J.A. Ten Cate et al, (*in preparation*)

[6] P.A. Johnson, B. Zinszner, P. N. J. Rasolofosaon, "Resonance and nonlinear elastic phenomena in rock", J. Geophys. Res., 1995 (*in review*).

[7] P.A. Johnson and P. N. J. Rasolofosaon, "Nonlinear elasticity and stress-induced anisotropy in rocks", J. Geophys. Res., 1995 (*in review*).

[8] Jeong K. Na and M.A. Breazeale, "Ultrasonic nonlinear properties of lead zirconate-titanate ceramics", J. Acoust. Soc. Am. **95**, 3213-3221 (1994).

[9] K. Van Den Abeele and M.A. Breazeale, "Theoretical model to describe dispersive nonlinear properties of Lead Zirconate-Titanate ceramics", J. Acoust. Soc. Am. 1995 (*in review*).

[10] R.A. Guyer, K.R. McCall and G.N. Boitnott, "Hysteresis, discrete memory and nonlinear wave propagation in rock", Phys. Rev. Lett. 1994 (*in review*).

[11] K.R. McCall and R.A. Guyer, "Equation of State and wave propagation in hysteretic nonlinear elastic materials", J. Geoph. Res. 1994 (*in review*).

[12] Hilbert, L. B., Jr., T. K. Hwong, N. G. W. Cook, K. T. Nihei, and L R. Myer, "Effects of strain amplitude on the static and dynamic nonlinear deformation of Berea sandstone", *Rock Mechanics Models and Measurements: Challenges From Industry*, P. P. Nelson and S. E. Laubach, Eds., A. A. Balkema, Rotterdam, 497-504, 1994.

[13] Birch, F., in *Handbook of Physical Constants* , Ed. Clark, S. P. , Jr., Geol. Soc. Am. Press, Connecticut, 97-174 (1966).

FIGURE CAPTIONS

Figure 1. Illustration of sandstone bar used in the MJGM experiment.

Figure 2. a) Source spectra as measured with a displacement probe for a 13.75 kHz drive at different amplitudes.

b) Spectra of propagated wave at receiver position 58 cm away from the source (from MJMG).

Figure 3. Simulation of source (left) and receiver (right) spectra at 58 cm for the amplitudes measured in Figure 2 for Q_L=60.

Arrows indicate the simulation results where β'=-250 and δ'=-3.2·10^{8}.

Figure 4. Simulation of source (left) and receiver (right) spectra at 58 cm for amplitudes measured in Figure 2 for Q_L=10.

Arrows again indicate simulation results. β' and δ' vary systematically with intensity.

Figure 5. Single iteration simulation for highest intensity level from Figure 4 using the same parameters as in Figure 4.

Figure 6. Simulation for highest intensity level from Figure 4 limiting calculations to a first order perturbation expression (taking into account only the influence of the first nonlinearity parameter β'=-300).

Figure 7. Simulated waveforms for displacement and acceleration corresponding to the spectra shown in Figure 4.

Figure 8: Typical stress-strain dependencies for large (big loop) and small (inner loop) static experiments illustrating distinct nonlinear response between both cases.

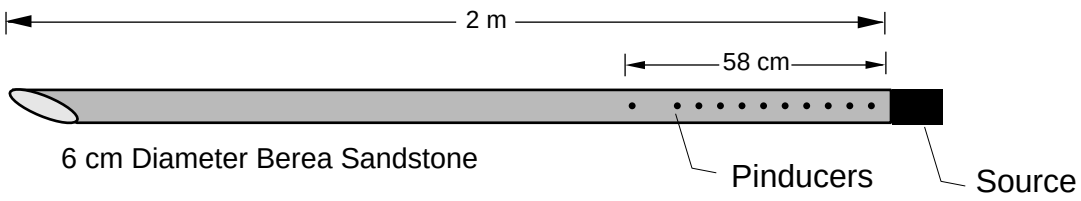

Figure 1
K. Van Den Abeele

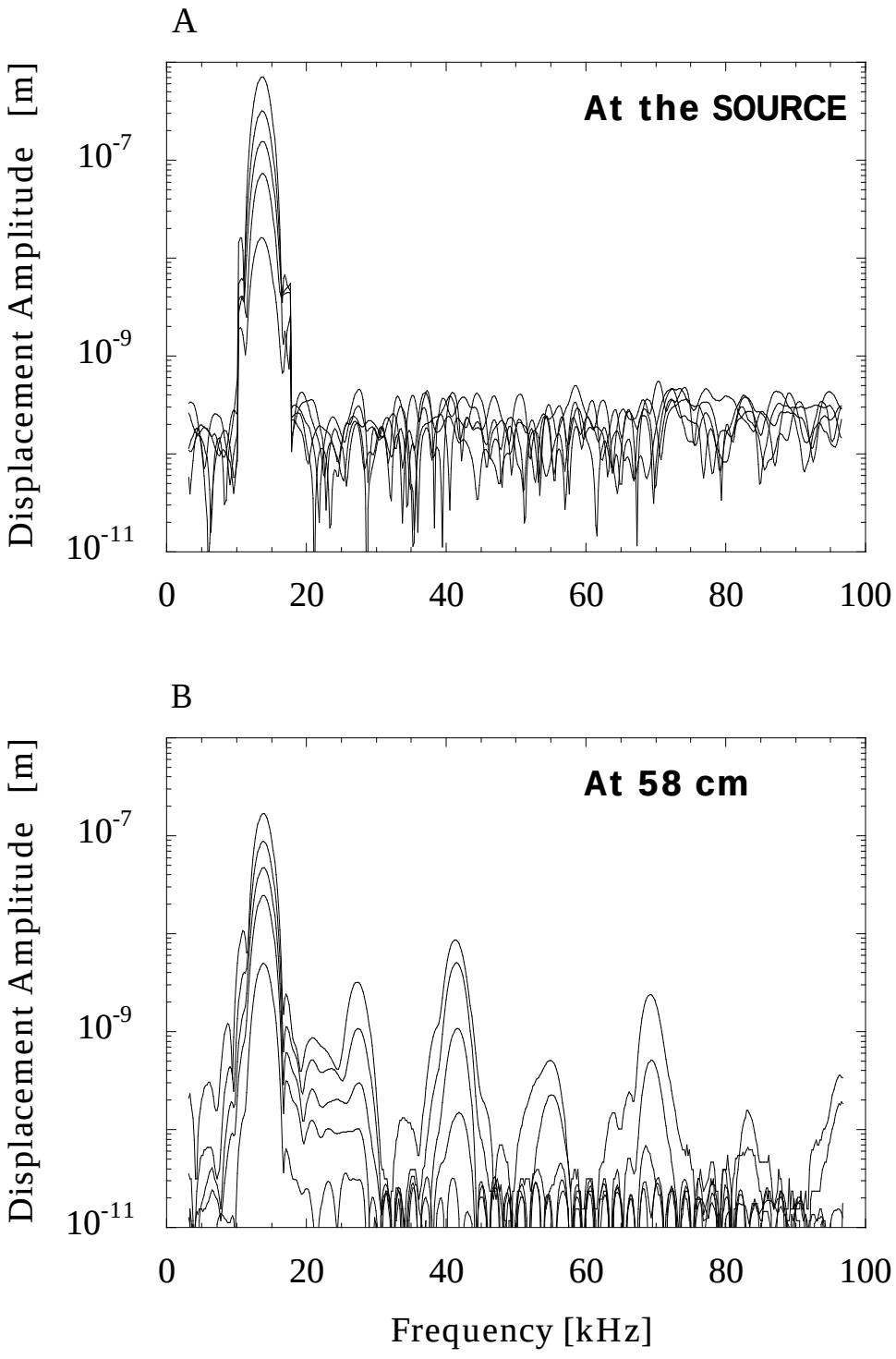
A
At the SOURCE
Displacement Amplitude [m]
10-7
10-9
10-11
0
20
40
60
80
100
B
At 58 cm
Displacement Amplitude [m]
10-7
10-9
10-11
0
20
40
60
80
100
Frequency [kHz]

Figure 2

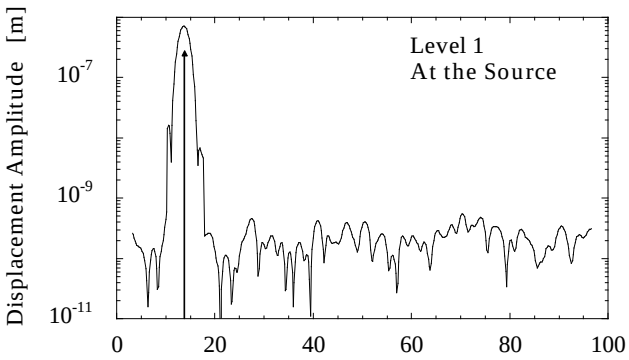
Displacement Amplitude [m]
Level 1
At the Source
10^{-7}
10^{-9}
10^{-11}
0
20
40
60
80
100

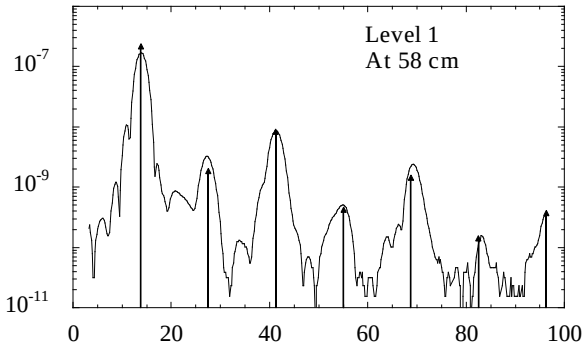
Level 1
At 58 cm
10^{-7}
10^{-9}
10^{-11}
0
20
40
60
80
100

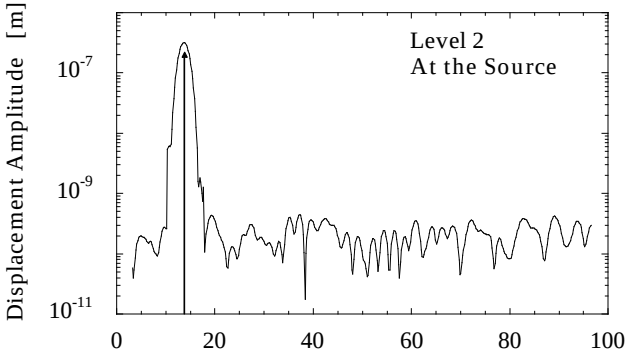
Displacement Amplitude [m]
Level 2
At the Source
10^{-7}
10^{-9}
10^{-11}
0
20
40
60
80
100

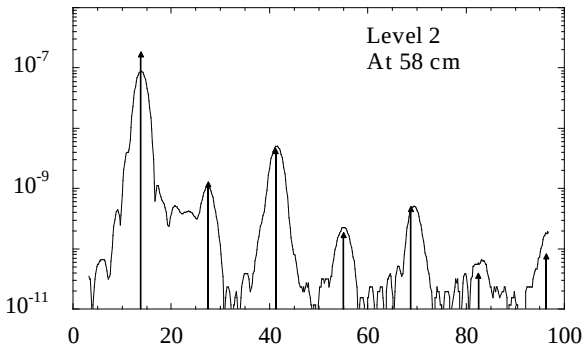
Level 2
At 58 cm
10^{-7}
10^{-9}
10^{-11}
0
20
40
60
80
100

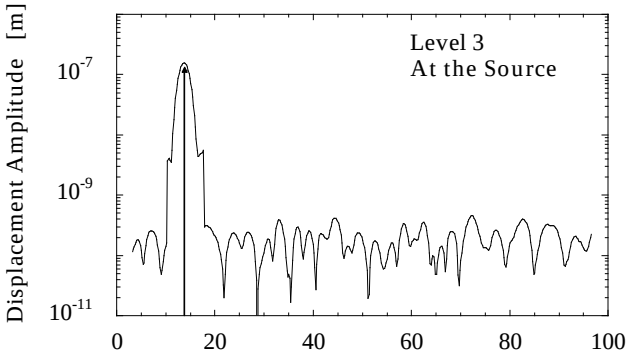
Displacement Amplitude [m]
Level 3
At the Source
10^{-7}
10^{-9}
10^{-11}
0
20
40
60
80
100

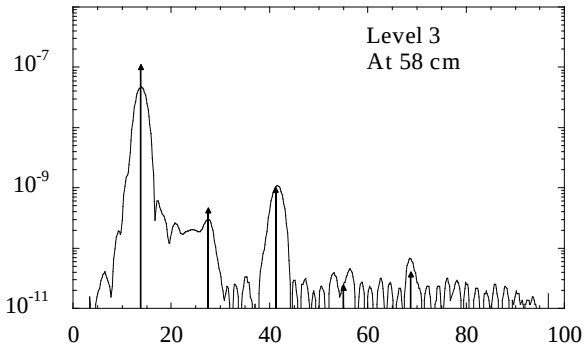
Level 3
At 58 cm
10^{-7}
10^{-9}
10^{-11}
0
20
40
60
80
100

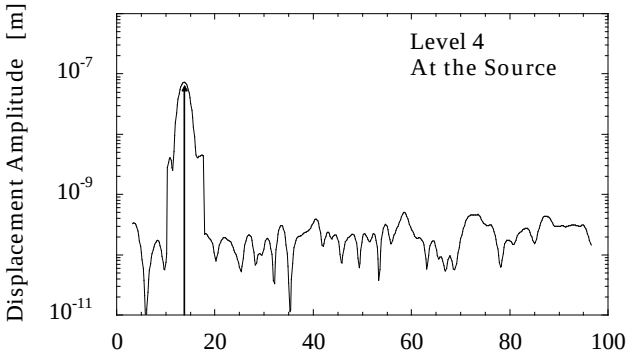
Displacement Amplitude [m]
Level 4
At the Source
10^{-7}
10^{-9}
10^{-11}
0
20
40
60
80
100

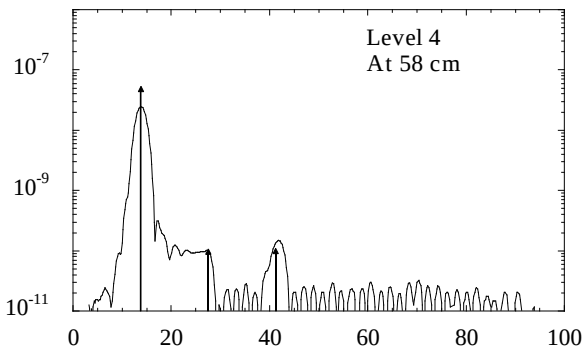
Level 4
At 58 cm
10^{-7}
10^{-9}
10^{-11}
0
20
40
60
80
100

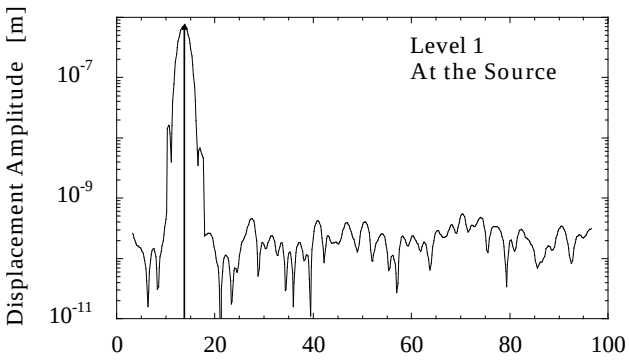
Displacement Amplitude [m]
Level 1
At the Source
10^{-7}
10^{-9}
10^{-11}
0
20
40
60
80
100

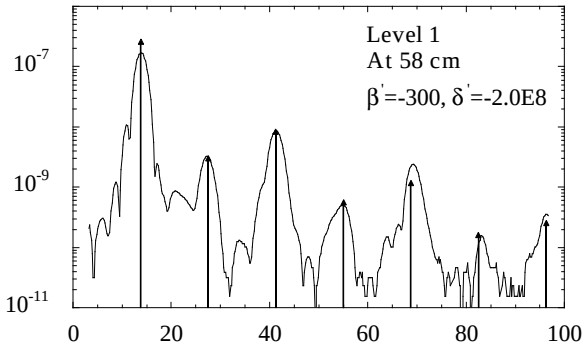
Level 1
At 58 cm
β'=-300, δ'=-2.0E8
10^{-7}
10^{-9}
10^{-11}
0
20
40
60
80
100

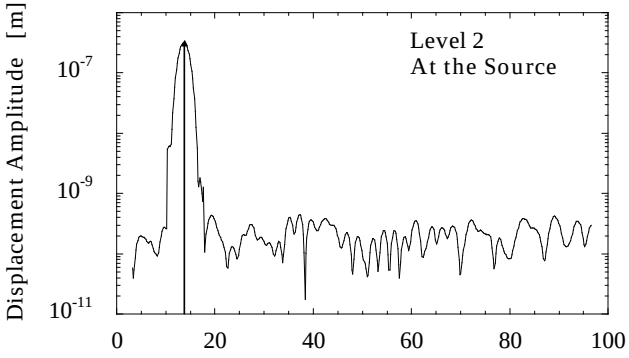
Displacement Amplitude [m]
Level 2
At the Source
10^{-7}
10^{-9}
10^{-11}
0
20
40
60
80
100

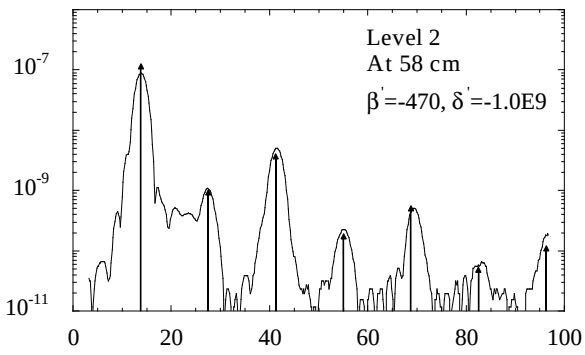
Level 2
At 58 cm
β'=-470, δ'=-1.0E9
10^{-7}
10^{-9}
10^{-11}
0
20
40
60
80
100

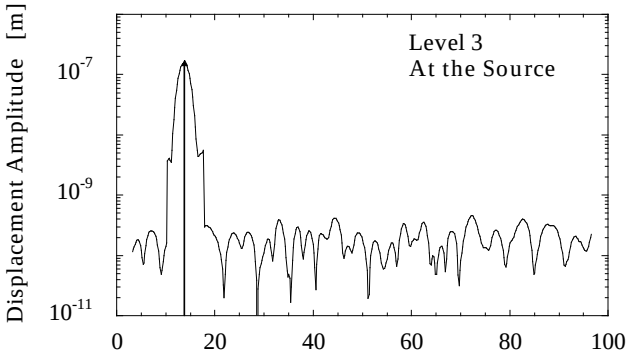
Displacement Amplitude [m]
Level 3
At the Source
10^{-7}
10^{-9}
10^{-11}
0
20
40
60
80
100

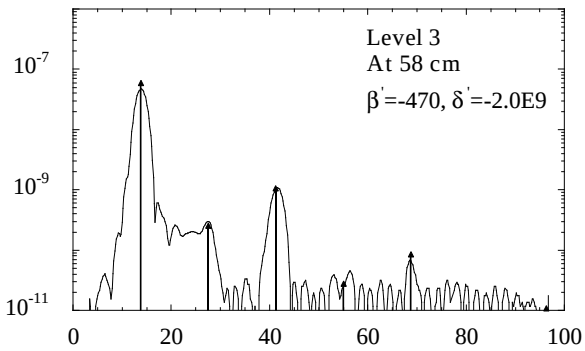
Level 3
At 58 cm
β'=-470, δ'=-2.0E9
10^{-7}
10^{-9}
10^{-11}
0
20
40
60
80
100

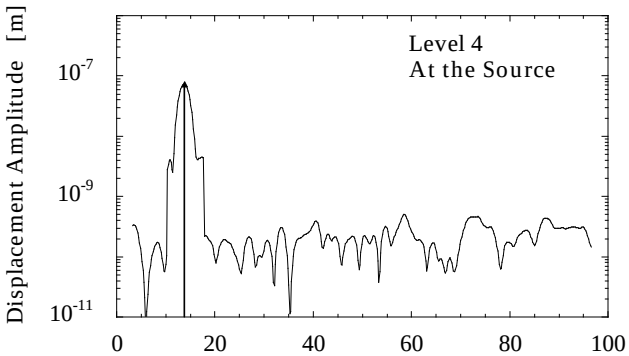
Displacement Amplitude [m]
Level 4
At the Source
10^{-7}
10^{-9}
10^{-11}
0
20
40
60
80
100

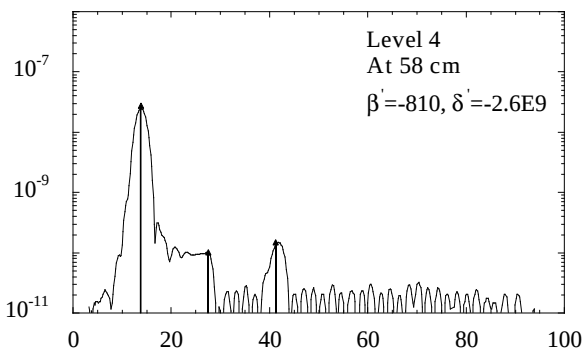
Level 4
At 58 cm
β'=-810, δ'=-2.6E9
10^{-7}
10^{-9}
10^{-11}
0
20
40
60
80
100

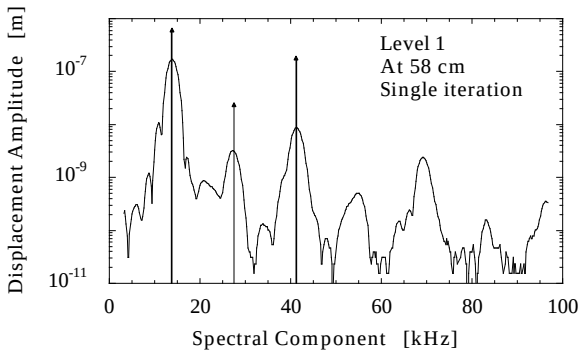
Displacement Amplitude [m]
10-7
10-9
10-11
0
20
40
60
80
100
Spectral Component [kHz]
Level 1
At 58 cm
Single iteration

Figure 5

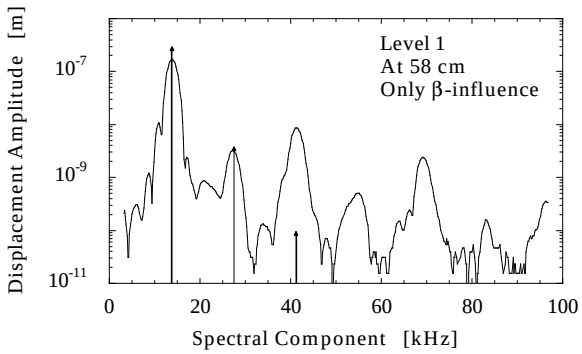
Displacement Amplitude [m]
10-7
10-9
10-11
0
20
40
60
80
100
Spectral Component [kHz]
Level 1
At 58 cm
Only β-influence

Figure 6

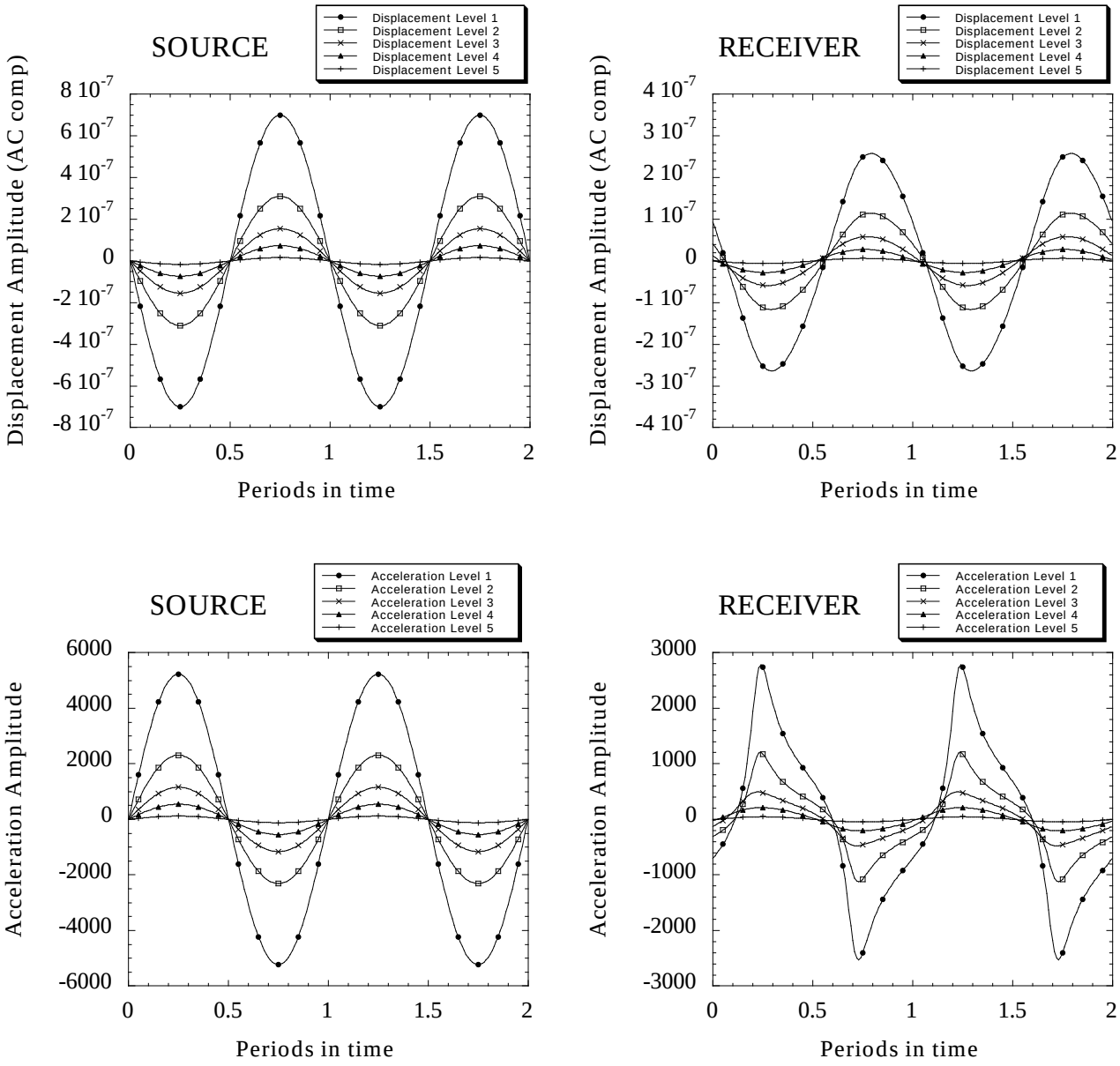
SOURCE
Displacement Level 1
Displacement Level 2
Displacement Level 3
Displacement Level 4
Displacement Level 5
Displacement Amplitude (AC comp)
8 10-7
6 10-7
4 10-7
2 10-7
0
-2 10-7
-4 10-7
-6 10-7
-8 10-7
0
0.5
1
1.5
2
Periods in time
RECEIVER
Displacement Level 1
Displacement Level 2
Displacement Level 3
Displacement Level 4
Displacement Level 5
Displacement Amplitude (AC comp)
4 10-7
3 10-7
2 10-7
1 10-7
0
-1 10-7
-2 10-7
-3 10-7
-4 10-7
0
0.5
1
1.5
2
Periods in time
SOURCE
Acceleration Level 1
Acceleration Level 2
Acceleration Level 3
Acceleration Level 4
Acceleration Level 5
Acceleration Amplitude
6000
4000
2000
0
-2000
-4000
-6000
0
0.5
1
1.5
2
Periods in time
RECEIVER
Acceleration Level 1
Acceleration Level 2
Acceleration Level 3
Acceleration Level 4
Acceleration Level 5
Acceleration Amplitude
3000
2000
1000
0
-1000
-2000
-3000
0
0.5
1
1.5
2
Periods in time

Figure 7

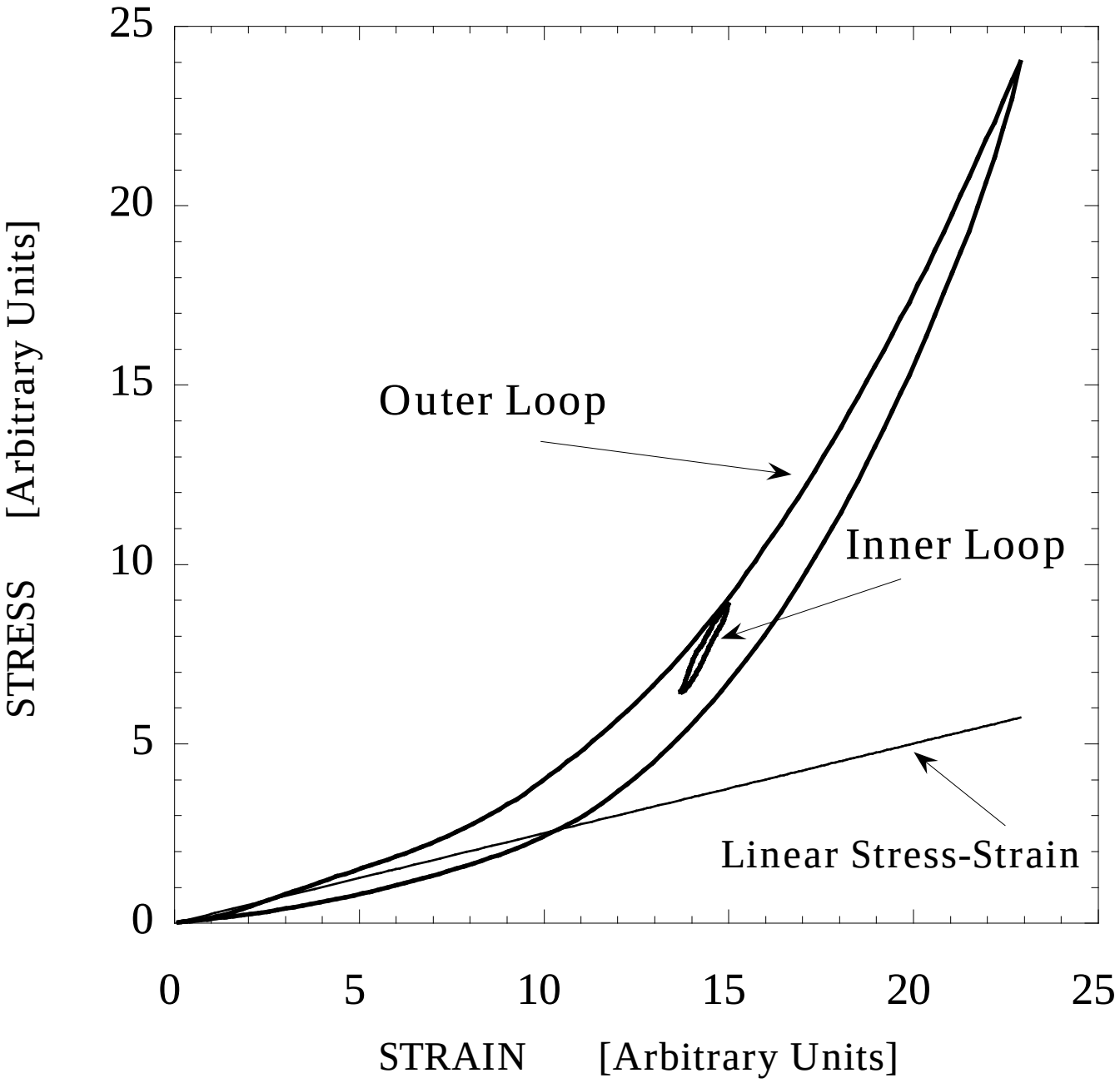
25
20
15
10
5
0
STRESS [Arbitrary Units]
Outer Loop
Inner Loop
Linear Stress-Strain
0
5
10
15
20
25
STRAIN [Arbitrary Units]